Report on the new EFOSC2 VPH grisms

Ivo Saviane
Lorenzo Monaco

February 20, 2008

1 Introduction

All data taken on February 13-14, and 14-15, 2008

2 Blue grism

To characterise the grisms the usual set of calibration frames were taken: bias frames, one arc frame, and dome flat-field frames. An example of raw arc and FF frames are shown in Fig. 6: it is evident that the right part of the CCD is not illuminated, because after passing through the VPHG the beam suffers a lateral deviation. This amounts to $84''$, or in other words, the usable field-of-view is reduced to $4'$. Fig. 7 shows a 2-D plot of the lines recognized in the raw arc, and the master arc after rectifying and wavelength calibrating. The frames have been trimmed down to 2021×1411 px. Ten lines are found by the search algorithm, which are shown in Fig. 8 and listed in Table 3. The table also shows that the maximum resolution is ~ 3200 at ~ 4700 Å, and also that the resolution is degraded at the extremes of the spectral range. Note that the FWHM spans several pixels, so using a $0\farcs3$ slit one could reach a resolution $R > 5000$. However a resolution of ~ 3000 is close to the theoretical limit (see Table 1), so only an empirical measurement can confirm this. Using these lines the wavelength calibration curve shown in Fig. 9 is obtained. The dispersion is 0.335 Å/px, and the spectrum covers the wavelength range from 4441 to 5114 Å. The highest dispersion of current EFOSC2 grisms is 1 Å/px, so the blue VPH grism offers a value three times larger than what is currently available. A plot of the wavelength calibrated arc is shown in Fig. 5.

3 Red grism

An example of raw arc and FF frames are shown in Fig. 6: in this case some reflections are visible in the arc frame, while the fringing pattern redder than 7000 Å is visible in the FF frame. For the red grism the non illuminated band has a width of $112''$, so the usable field-of-view is only $3.5'$. Fig. 7 shows a 2-D plot of the lines recognized in the raw arc, and the master arc after rectifying and wavelength calibrating. The frames have been trimmed down to 2021×1231 px. Several lines are found by the search algorithm, and 23 of them are used for the wavelength calibration. They are shown in Fig. 8 and listed in Table 3. The table also shows that the maximum resolution is ~ 3400 at ~ 6600 Å, and also that the resolution is degraded at the extremes of the spectral range. Note that the FWHM spans several pixels, so using a $0\farcs3$ slit one could reach a resolution $R > 5000$. However a resolution of ~ 3000 is close to the theoretical limit (see Table 1), so only an empirical measurement can confirm this. Using these lines the wavelength calibration curve shown in Fig. 9 is obtained. The dispersion is 0.546 Å/px, and the spectrum covers the wavelength range from 6047 to 7147 Å. The highest dispersion of current EFOSC2 grisms is 1 Å/px, so the red VPH grism offers a value two times larger than what is currently available. A plot of the wavelength calibrated arc is shown in Fig. 10.

Table 1: Comparison of expected performance of Golem VPHGs, and measured parameters of VPHGs provided by Vik Dhillon.

	lines mm^{-1}	λ_{min} Å	λ_{cen} Å	λ_{max} Å	RS	Å px^{-1}	FWHM Å	bin	slit
G2	2118	4870	5100	5340	3500	0.23	1.45		$1''$
VR	1557	4441	4777	5114	3200	0.34	1.5	1	$0''.5$
					3200	0.67	1.5	2	$0''.5$
					2200	0.67	2.1	2	$1''$
G4	1570	6220	6560	6920	3000	0.34	2.18		$1''$
VB	1070	6047	6597	7147	3400	0.55	2.0	1	$0''.5$
					3000	1.08	2.2	2	$0''.5$
					2000	1.09	3.3	2	$1''$

Notes:
G2: Golem/ 2h, [O III] 5007, Mg 5200
G4: Golem/ 4h, Hα 6563
VR: 'Vik' 475
VB: 'Vik' 656

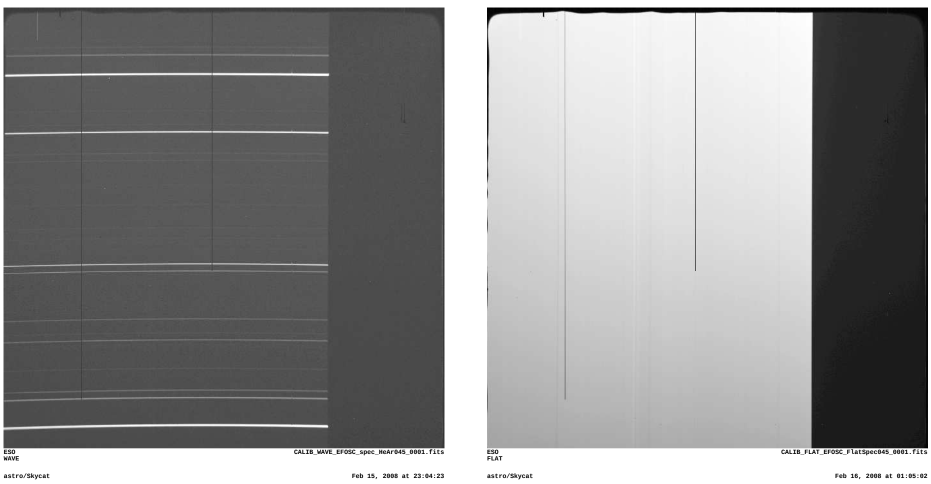

Figure 1: Raw arc and FF of the blue grism

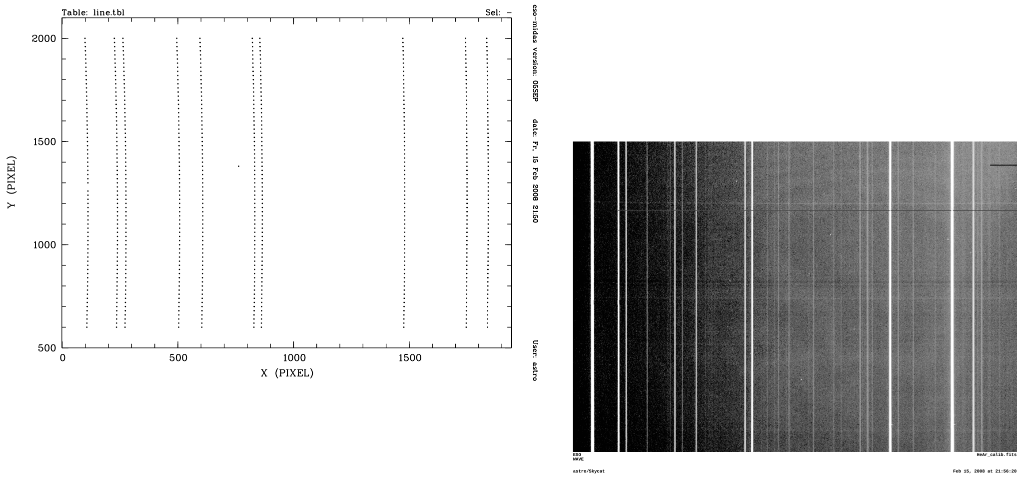

Figure 2: The lines found by the search algorithm are displayed in the left panel, and the master arc after calibration is shown in the right panel.

λ[Å]	ION	FWHM	R	n(px)	COMMENTS
4471.4790	HE I	2.184	2047	6.519	
4510.7334	AR I	1.818	2481	5.427	
4522.5890		1.748	2587	5.218	No stdline at this lambda
4545.0518	AR II				so maybe it's this Ar II?
4589.8979	AR II	1.717	2677	5.125	
4628.4409	AR I	1.518	3049	4.531	
4702.3262	AR I	1.471	3197	4.391	*
4713.1455	HE I	1.497	3148	4.469	
4921.9312	HE I	1.644	2994	4.907	
5015.6797	HE I	1.800	2786	5.373	
5047.7378	HE I	2.187	2308	6.528	

Table 2: For each arc line we list its identification and some characteristic parameters. R is the resolution for a $0\farcs5$ slit, and n(px) is one FWHM expressed in pixels.

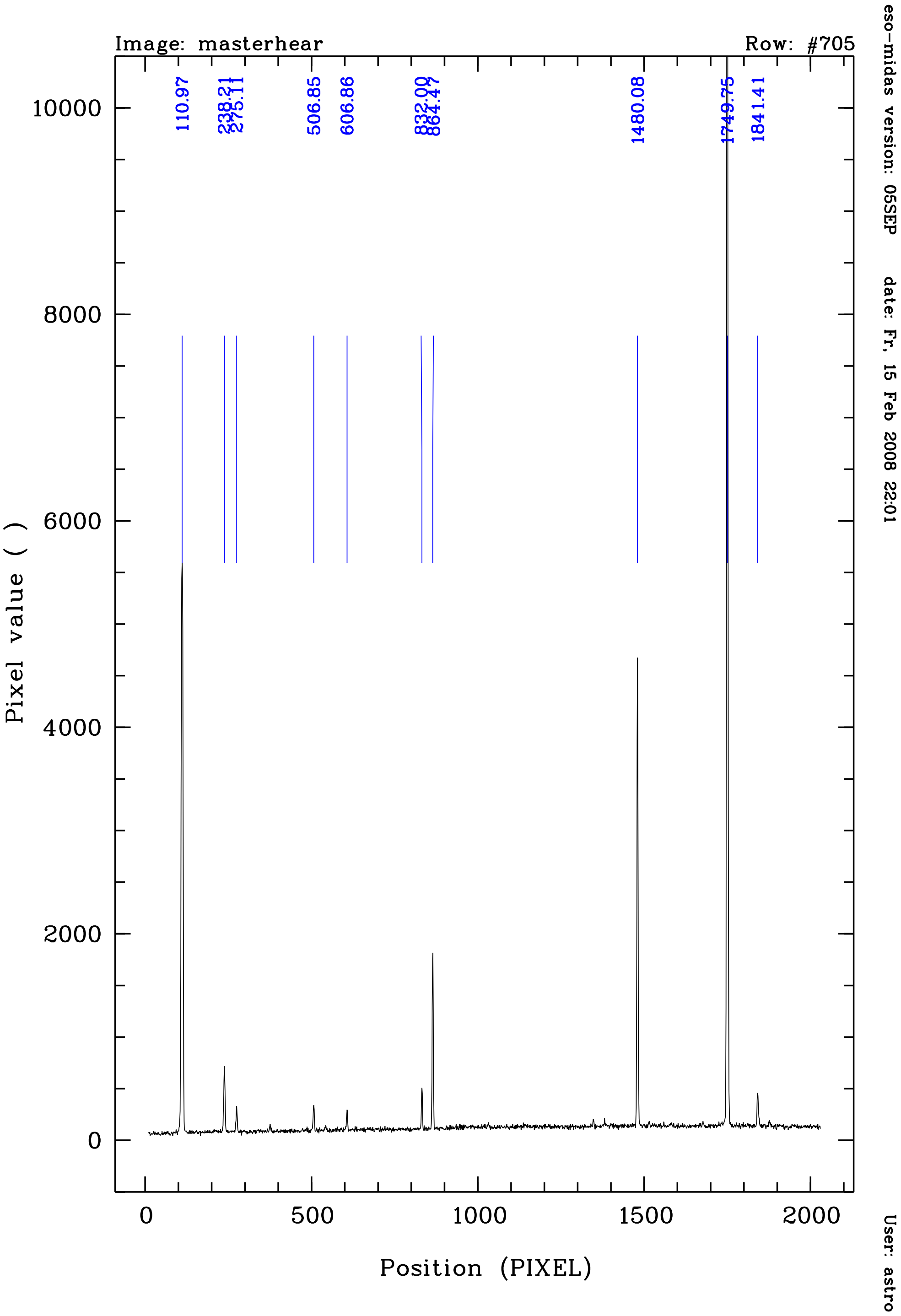

Figure 3: The ten arc lines marked on a trace of the arc spectrum.

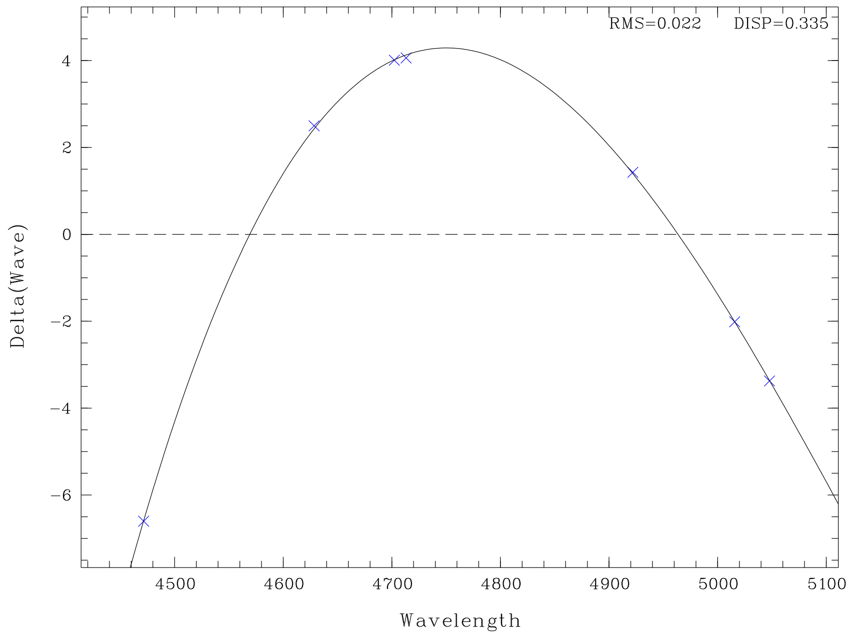

Figure 4: The wavelength calibration curve of the blue VPH grism.

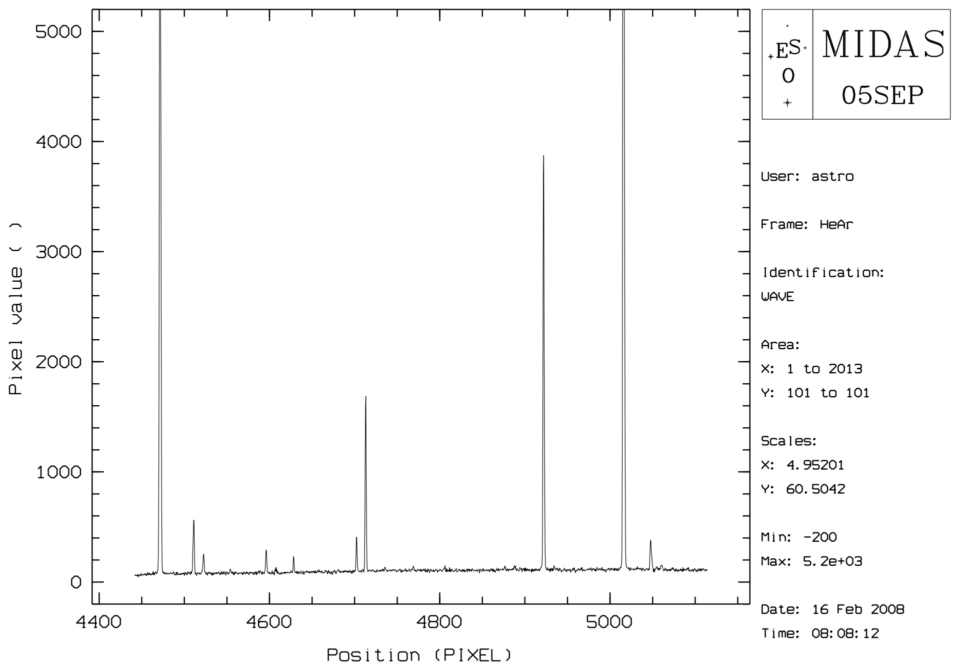

Figure 5: A trace of a blue arc after wavelength calibration

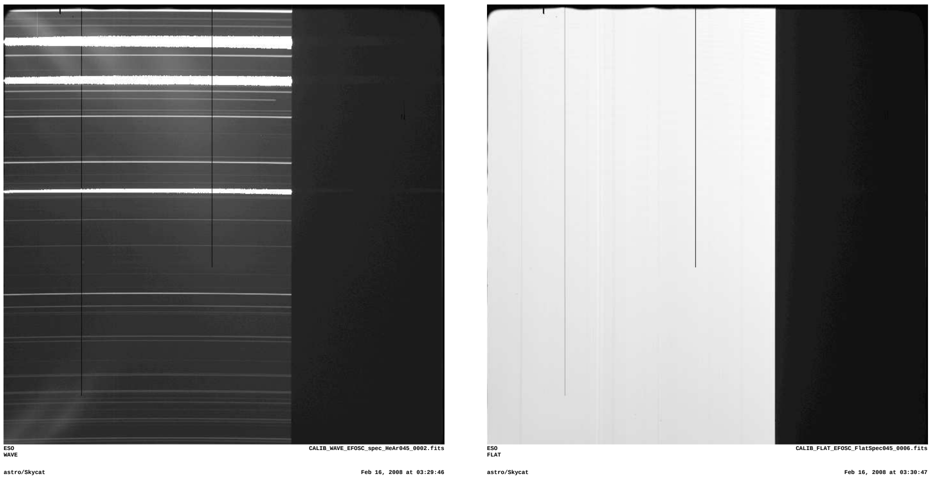

Figure 6: Raw arc and FF of the red grism

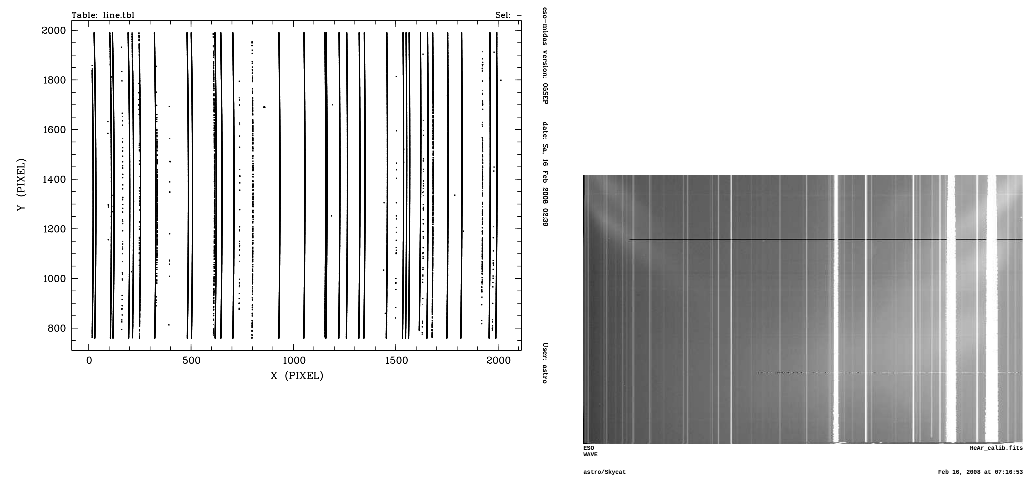

Figure 7: The lines found by the search algorithm on the red grism are displayed in the left panel, and the master arc after calibration is shown in the right panel.

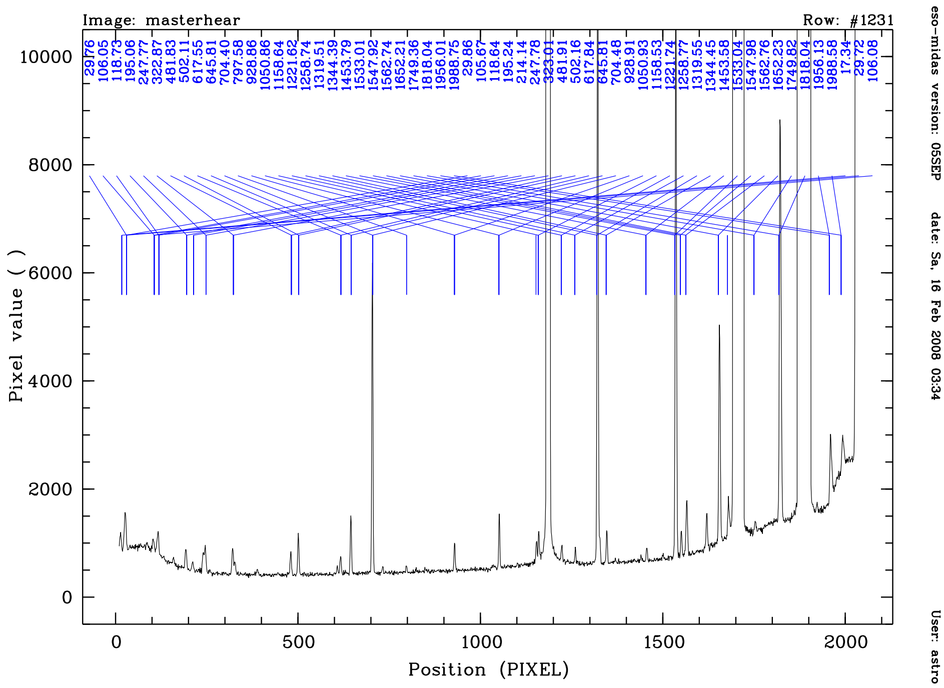

Figure 8: The arc lines marked on a trace of the red arc spectrum.

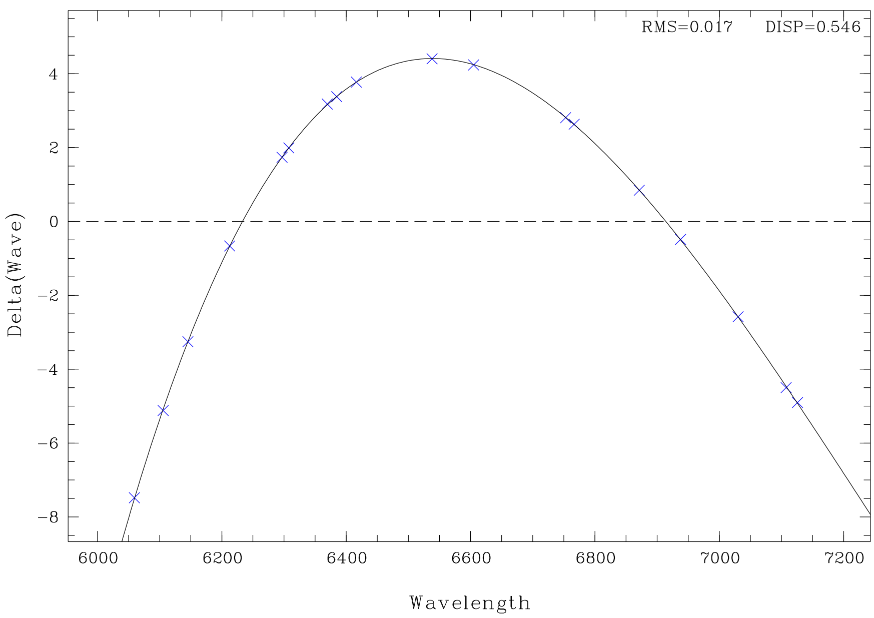

Figure 9: The wavelength calibration curve of the red VPH grism.

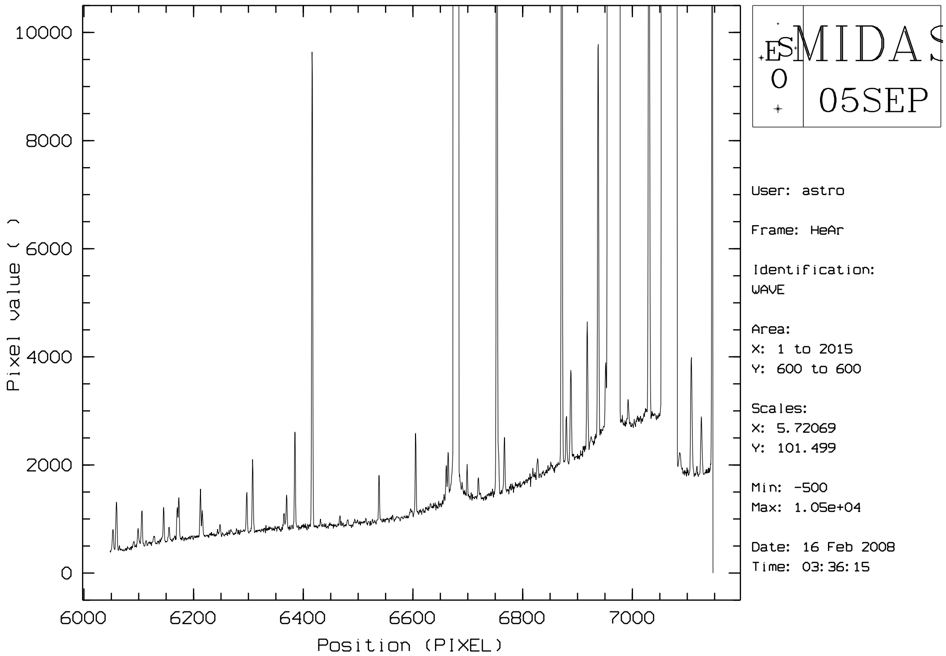

Figure 10: A trace of a red arc after wavelength calibration

λ[Å]	ION	FWHM	R	n(px)	COMMENTS
6059.3726	AR I	2.134	2839	3.908	
6105.6353	AR I	2.370	2576	4.341	
6145.4409	AR I	2.342	2624	4.289	
6172.2778	AR II				sat
6212.5029	AR I	2.202	2821	4.033	
6296.8721	AR I	2.120	2970	3.883	
6307.6572	AR I	1.985	3178	3.636	
6369.5747	AR I	1.774	3590	3.249	
6384.7168	AR I	2.011	3175	3.683	
6416.3071	AR I	1.988	3228	3.641	
6466.5527	AR I	1.915	3377	3.507	
6538.1118	AR I	1.934	3381	3.542	
6604.8535	AR I	1.999	3304	3.661	
6678.1509	HE I				sat
6752.8335	AR I	2.011	3358	3.683	
6766.6118	AR I	1.997	3388	3.658	
6871.2891	AR I	2.059	3337	3.771	
6937.6641	AR I	2.228	3114	4.081	
6965.4307	AR I				sat
7030.2515	AR I	2.436	2886	4.462	
7065.1899	HE I				sat
7107.4780	AR I	2.802	2537	5.132	
7125.8198	AR I	2.796	2549	5.121	

Table 3: For each red arc line we list its identification and some characteristic parameters. R is the resolution for a $0\farcs5$ slit, and n(px) is one FWHM expressed in pixels.

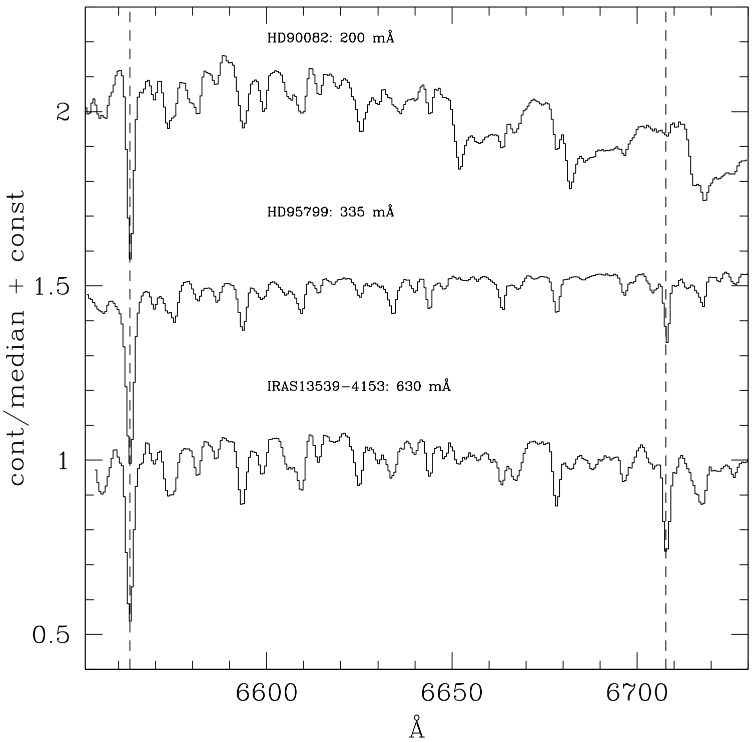

Figure 11: A portion of the spectrum of three stars with different EWs of the lithium $\lambda 6707.8$ line. The spectra have been obtained with the red VPHG, and the dashed vertical segments mark the position of Hα and the lithium line.

4 Efficiencies

Get the following macros and turn response functions into efficiencies. Note that the night was not photometric, so you will get only a lower limit.

```
-- DVD-efosc2-aug-2003 -- ./EFOSC2_Aug_2003/from_w3p6off/Gr9/efficiency.mac
-- DVD-efosc2-aug-2003 -- ./EFOSC2_Aug_2003/Gr13/efficiency.mac
```

5 A couple of science cases

5.1 Measurement of lithium line $\lambda 6707.8$

Measuring the lithium abundance in stars is important because xxx. This abundance is routinely measured using the line at 6707.8 Å. To test the feasibility of such a measurement, we took spectra of three stars with different EWs of the lithium line. The extracted and continuum-normalized spectra are shown in Fig. 11, and they have SNRs better than 50. Clearly EWs down to 300 mÅ can be easily measured, while the 200 mÅ star is more ambiguous, because of its late spectral type. The line is probably detected, but a confirmation with an earlier type star is needed.

5.2 Rotation curves of spiral galaxies

Rotation curves of spiral galaxies are used to study their kinematics, in the search for the amount and distribution of dark matter, which are constrained by departures from the expected curve of

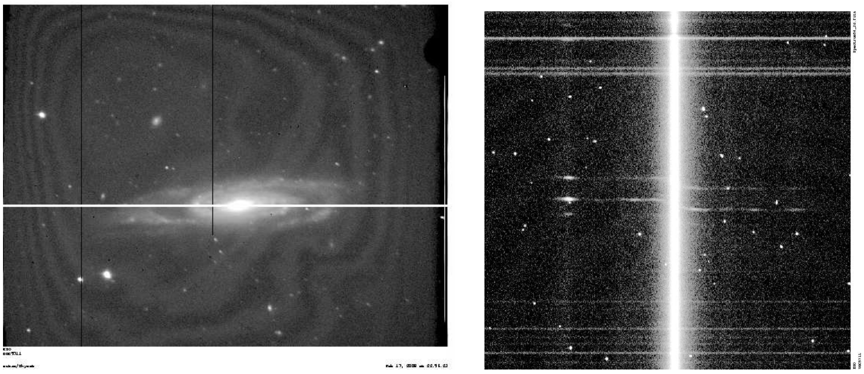

Figure 12: The left panel contains the acquisition image of UGC 5711 in white light, showing the location of the slit across the galaxy. The right panel shows the wavelength-calibrated and distortion-free spectrum in the region of Hα. The wavelength increases upwards.

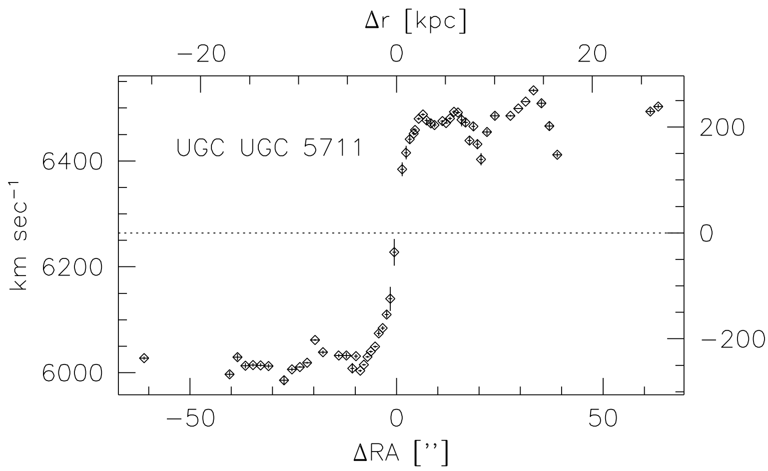

Figure 13: The rotation curve of UGC 5711 measured with the red VPHG. The dotted line shows the recession velocity of 6264 km sec^{-1} from RC3. The physical radius has been computed assuming $H_0 = 72$ km sec^{-1} Mpc^{-1}.

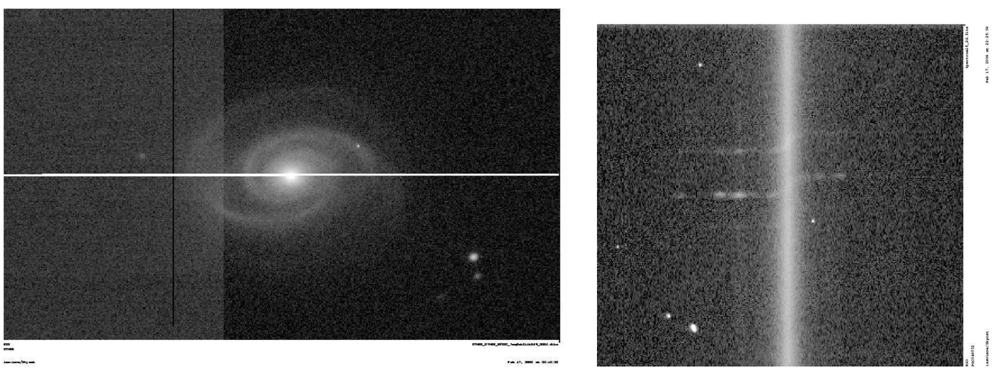

Figure 14: The slit position across PGC 048532 is shown in the R-band acquisition image (left panel), while the right panel shows the wavelength-calibrated and distortion-free spectrum in the region of Hα. The wavelength increases upwards.

Figure 15: The rotation curve of PGC 048532 measured with the red VPHG. The dotted line shows the recession velocity of xxx km sec^{-1} from RC3. The physical radius has been computed assuming $H_0 = 72$ km sec^{-1} Mpc^{-1}.

a rotating disk. These also offer clues on the role of interactions and their impact on evolutionary histories. Galaxy evolution in general can also be explored by comparing rotation curves of distant galaxies with those of nearby objects.

Rotation curves derived from emission lines, and in particular those of Hα and [N II] are particularly useful to derive the mass distribution in disk galaxies, because they trace the motion of interstellar gas of the young populations. This has a velocity dispersion (of the order of 5–10 km s^{-1}) that is much smaller than its rotational velocity, allowing accurate measurements. Among spiral galaxies, giant spirals seems to be the best laboratories to study the structure and kinematics (see Fig...). They have extended disks and rotational velocities of ~ 400 km s^{-1}. Through their rotational curves we can study the cusp/core and angular momentum problems (ref. xxx) and the DM distribution on the 100 kpc scale.

To measure rotation curves of giant spiral galaxies we took spectra of two objects with the red VPHG. The first piece of data is a 1200 sec spectrum of the giant spiral UGC 5711, with the slit oriented along its major axis (see Fig. 12). A portion of the 2D spectrum near Hα is shown in Fig. 12. The differential velocity can be easily seen on the frame, and the rotation curve is plotted in Fig. 13. The figure shows that the systemic velocity is compatible with that of the RC3 catalog, and that the precision we obtain is comparable to that of standard studies of this kind xxx.

The same exercise was done with PGC 048532, for which the slit position and 2D spectrum are shown in Fig. 14. The rotation curve displayed in Fig. 15 is xxx

6 Problems

- FF red has BIG gradient => response function depends on position in the slit; 33000 -> 42700 / 1220 px -> // 8 ADU/px
- FF blue has BIG gradient => response function depends on position in the slit; gradient is 22800 -> 32000 // 6 ADU/px
- 2nd order contamination in red grism
- The spectral range of the blue grism does not reach the Mg 5200 triplet

6.1 Alain

Dear Colleagues,

The new grism for Efosc gave some difficulties partially solved. Both ones are within specs for the dispersion, central wavelength. The effciency still must be confirmed by Vik. Both ones presented strong parasitic stray light for the calibration exposures either FF or arc. This stray light is produced by the inside metallic black painted part of the cylinder holder not covered by the prism itself. Installing black velvet tape we managed to suppress all this parasitic light. Both ones introduce a lateral shift of the image field (perpendicular to the dispersion). The 656 VPH with an higher shift value. This effect is produced by a mismatch error between the prism and grating dispersion axis. A VPH grism in Paranal also suffered the same defect The ultraspec dectector now installed on Efosc has a much smaller field of view and tests on the normal mode of Efosc using the CCD#40 must be done to check the shift effect on a larger field.

Acknowledgements

We thank I. Yegorova and A. Pizzella for computing the kinematic data of the spiral galaxies.